A MITE Transposon Insertion Is Associated with Differential Methylation at the Maize Flowering Time QTL *Vgt1*

Sara Castelletti,*[,1] Roberto Tuberosa,* Massimo Pindo,[†] and Silvio Salvi*[,2]
*Department of Agricultural Sciences (DipSA), University of Bologna, Bologna, and [†]Research and Innovation Centre, Foundation Edmund Mach, San Michele all'Adige, Trento, Italy

ABSTRACT One of the major quantitative trait loci for flowering time in maize, the *Vegetative to generative transition 1* (*Vgt1*) locus, corresponds to an upstream (70 kb) noncoding regulatory element of *ZmRap2.7*, a repressor of flowering. At *Vgt1*, a miniature transposon (MITE) insertion into a conserved noncoding sequence was previously found to be highly associated with early flowering in independent studies. Because cytosine methylation is known to be associated with transposons and to influence gene expression, we aimed to investigate how DNA methylation patterns in wild-type and mutant *Vgt1* correlate with *ZmRap2.7* expression. The methylation state at *Vgt1* was assayed in leaf samples of maize inbred and F_1 hybrid samples, and at the syntenic region in sorghum. The *Vgt1*-linked conserved noncoding sequence was very scarcely methylated both in maize and sorghum. However, in the early maize *Vgt1* allele, the region immediately flanking the highly methylated MITE insertion was significantly more methylated and showed features of methylation spreading. Allele-specific expression assays revealed that the presence of the MITE and its heavy methylation appear to be linked to altered *ZmRap2.7* transcription. Although not providing proof of causative connection, our results associate transposon-linked differential methylation with allelic state and gene expression at a major flowering time quantitative trait locus in maize.

KEYWORDS
DNA methylation
gene regulation
conserved noncoding sequences
Zea mays

Methylation of cytosine residues is one of the most extensively studied epigenetic modifications of DNA. It is widespread in many eukaryotic organisms ranging from fungi to higher plants (Feng *et al.* 2010; Jones 2012). To investigate the role of genic and intergenic methylation, high-resolution DNA methylation analysis has been performed or is underway in many plant species (Zhang *et al.* 2006; Zilberman *et al.* 2007; Cokus *et al.* 2008; Lister *et al.* 2008; Zemach *et al.* 2010; Eichten *et al.* 2011; Li *et al.* 2012; Gent *et al.* 2013). Many of these have shown that transposable elements are highly methylated, which supports the hypothesis that methylation is a strategy to repress TEs mobility (Lippman *et al.* 2003; Zhang *et al.* 2006). Methylation also plays a major role in regulating gene expression and, in general, methylation of promoter sequences has been negatively correlated with transcriptional activity (Zhang *et al.* 2010).

In plants, several studies have highlighted the correlation between epigenetic modifications and heritable phenotypic variation. The presence of 853-bp tandem repeats located 100 kb upstream from the *b1* gene is essential for paramutation (Brink 1958) to occur at the *b1* locus in maize; the methylation state of the repeats correlates with the epigenetic state of the *b1* coding region, which also involves an RNA-mediated mechanism (Stam *et al.* 2002; Arteaga-Vazquez *et al.* 2010). In *Linaria vulgaris*, the methylation state of the *Lcyc* gene was shown to be responsible for a naturally available developmental mutant for flower symmetry (Cubas *et al.* 1999). In melon, the insertion of a DNA transposon in the *CmWIP1* locus, encoding a C2H2 zinc-finger transcription factor, determines hypermethylation of the gene promoter, which in turn results in the formation of female flowers (Martin *et al.* 2009). Telias *et al.* (2011) showed that variegation in apple

doi: 10.1534/g3.114.010686
Manuscript received November 12, 2013; accepted for publication February 26, 2014; published Early Online March 7, 2014.

Supporting information is available online at http://www.g3journal.org/lookup/suppl/doi:10.1534/g3.114.010686/-/DC1
Raw data were deposited in the Sequence Read Archive under accession numbers: maize SRX469305 and sorghum SRX469306.
[1]Present address: UMR de Génétique Végétale INRA − Univ Paris-Sud − CNRS, Gif-sur-Yvette, France.
[2]Corresponding author: Department of Agricultural Sciences (DipSA), University of Bologna, Viale Fanin 44, 40127 Bologna, Italy. E-mail address: silvio.salvi@unibo.it

skin is dependent on differential methylation of the promoter of a myb transcription factor (*MYB10*), which is a key regulator of anthocyanin biosynthesis. On a larger scale, the development of a population of epigenetic recombinant inbred lines in *Arabidopsis thaliana* showed that stably inherited DNA methylation changes are indeed associated with heritable variation for two complex traits, namely flowering time and plant height (Johannes *et al.* 2009).

Flowering time is a key trait for crop adaptation to different cultivation environments and maize is no exception. Genetic dissection of this trait has been the topic of several QTL studies in maize, as the nature of the variability for flowering time is prevalently quantitative (Chardon *et al.* 2004; Buckler *et al.* 2009; Salvi *et al.* 2009; Tuberosa and Salvi 2009). One of the major flowering-time QTL, *Vegetative to generative transition 1* (*Vgt1*) (Phillips *et al.* 1992; Vlăduţu *et al.* 1999; Salvi *et al.* 2002) on chromosome 8, corresponds to a ≈2-kb intergenic region upstream of an *Ap2*-like flowering-time gene, *ZmRap2.7* and appears to act as a *cis*-regulator of *ZmRap2.7* expression (Salvi *et al.* 2007). A maize–sorghum–rice evolutionarily conserved noncoding sequence (CNS) (Freeling and Subramaniam 2009) was identified within *Vgt1*; in early *Vgt1* alleles, this CNS is interrupted by the insertion of a miniature transposon (MITE) belonging to the Tourist family (Salvi *et al.* 2007), and this insertional polymorphism has been repeatedly identified as strongly associated with flowering time in independent studies (Salvi *et al.* 2007; Ducrocq *et al.* 2008; Buckler *et al.* 2009; Hung *et al.* 2012; Truntzler *et al.* 2012).

In this work, we compared the DNA methylation state of two *Vgt1* alleles to investigate a possible role for epigenetic changes at *Vgt1* in the regulation of *ZmRap2.7* expression in the context of a putative *cis*-interaction between the two loci. We focused in particular on the CNS/MITE region with the objective of improving our understanding of the involvement of conserved DNA elements in determining phenotypic variation.

MATERIALS AND METHODS

Plant materials

Seedlings of B73, Gaspé Flint, N28, C22-4, R22, and N28xC22-4 F_1 hybrid were grown in a greenhouse at 25° under long-day photoperiod. B73 is the reference genotype for the maize community (Wei *et al.* 2007; Schnable *et al.* 2009), N28 is a dent line belonging to the Nebraska Stiff Stalk Synthetic group. The strain C22–4 is nearly isogenic to N28 and carries the early *Vgt1* allele in an ≈7-cM introgression originating from the maize variety Gaspé Flint characterized by extreme earliness (Vlăduţu *et al.* 1999). R22 is an N28 nearly isogenic line derived from the cross between N28 and C22-4 (Salvi *et al.* 2007). For all experiments (methylation analysis and expression analysis), leaf tissue was harvested at four developmental stages: first leaf (V1), third leaf (V3), fifth leaf (V5), and seventh leaf (V7), fully expanded, according to the classification reported in (Ritchie *et al.* 1993); after the collection of leaves, ligule, leaf tip, and midrib vein were removed to keep only leaf blade; tissues from 15 different plants were pooled for each genotype and stage of development. For each genotype and stage of development, two biological replicates were grown and harvested. One additional N28-nearly isogenic line, R66 (as described in Salvi *et al.* 2007) was grown and sampled to be included in methylation analysis (see File S1).

Sorghum B.Tx623 seedlings (seeds kindly provided by William Rooney, Texas A&M University) were grown in a growth chamber in controlled conditions (25°, 16-hr photoperiod). Leaves were harvested from 15 seedlings grown in two reps, at two developmental stages (first leaf, V1 and seventh leaf, V7, fully expanded), and only leaf blades were collected.

ZmRap2.7 expression analysis

Total RNA was isolated from leaf tissues by use of TRI Reagent (Sigma-Aldrich, St. Louis, MO). Complementary (c)DNA was synthesized with the High Capacity cDNA Reverse Transcription Kit (Applied Biosystems, Foster City, CA). Real-Time polymerase chain reactions (PCRs) were set up using cDNA as template and Platinum SYBR Green qPCR SuperMix-UDG (Invitrogen, Carlsbad, CA) and performed on a 7500 Fast Real-Time PCR System (Applied Biosystems, Foster City, CA) with the following thermocycling conditions: 40 cycles at 95° for 10" and 64° for 1'; primers for the target gene *ZmRap2.7* (Salvi *et al.* 2007) and the housekeeping gene *aat* (alanine aminotransferase, housekeeping gene) (Woodhouse *et al.* 2006) were used (Table S1). Relative gene expression was calculated following the ΔΔCt method (Livak and Schmittgen 2001).

Bisulfite treatment

Genomic DNA was extracted following a standard CTAB method as described in (Saghai-Maroof *et al.* 1984). For each sample, 500 ng of genomic DNA from N28, C22-4, and N28 x C22-4 F_1 leaves at V1, V3, V5, and V7 stages and from sorghum B.Tx623 leaves at V1 and V7 stages was treated using EZ DNA Methylation-Gold kit (Zymo Research, Orange, CA) following the manufacturer's instructions.

Amplicon ultra-deep sequencing

Degenerate primers targeting the CNS/MITE region in maize (Figure 1 and Table S1) and the CNS region in sorghum B.Tx623 (Table S1) were designed using the Kismeth software (Gruntman *et al.* 2008). For maize samples, 4 μL of bisulfite-treated genomic DNA was PCR-preamplified with AmpliTaq Gold DNA Polymerase (Applied Biosystems). All the 16 PCR products were quantified by Nanodrop 3300 Fluorospectrometer (Thermo Scientific, Wilmington, DE) using the Quant-iT PicoGreen dsDNA Assay Kit (Invitrogen). The MITE and CNS amplicons were pooled according to the stage of development, and eight different libraries were generated employing the GS-FLX Titanium Rapid Library Preparation Kit following the manufacturer's recommendations (454 Life Sciences, Branford, CT). To overcome the limitation in the number of samples that can be sequenced in parallel, the Multiplex Identifier was used. For sorghum, after a first preamplification on bisulfite-treated genomic DNA, 1 μL of nonpurified PCR product was used as template in a second nested amplification performed with fusion primers composed of three parts: (i) 454-specific adaptors (A and B), (ii) 10-bp Multiplex Identifier to barcode the samples, and (iii) sequence-specific primers (Table S1); the thermocycling conditions were 30 cycles at 95° for 30", 49° for 30", and 72° for 45". The final double-stranded DNA libraries were quantitated via quantitative (q)PCR using Library quantification kit–Roche 454 Titanium (KAPA Biosystems, Boston, MA) prior to emulsion PCR amplification. Pyrosequencing was performed on a GS FLX instrument (454; Life Sciences) according to the manufacturer's recommendations. Processed and quality-filtered reads were analyzed with the Kismeth software (Gruntman *et al.* 2008), and statistical significance was tested with analysis of variance. The achieved average depth of sequencing was 1591X for the CNS region in N28, 857X for the CNS/MITE region in C22-4, and 108X for the CNS region in sorghum B.Tx623. Raw data were deposited in the Sequence Read Archive under accession numbers: maize SRX469305 and sorghum SRX469306.

Methylation quantification with Mutation Surveyor

Two different genomic regions within *Vgt1* (Ampl Bis-Sanger from N28 and C22-4 and CNS/MITE from N28 x C22-4 F_1, Figure 1 and

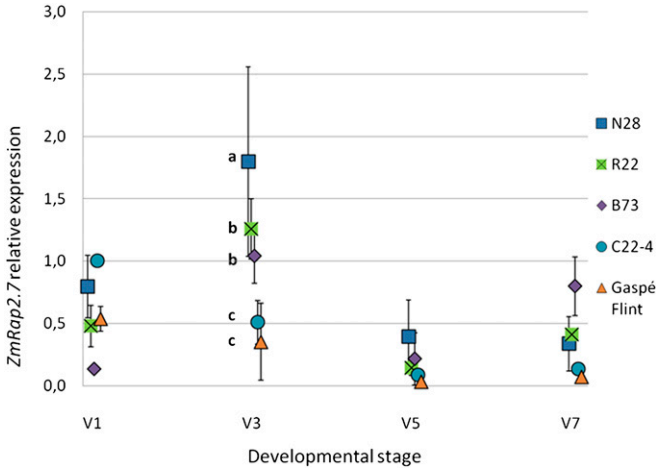

Figure 1 *ZmRap2.7* expression analysis across four developmental stages (V1, V3, V5, and V7) on five maize lines used in this study. Gene expression levels (mean values) are expressed relatively to the *aat* housekeeping gene. Standard deviation values are shown as bars; different letters (a−c) indicate significant difference ($P < 0.01$, Fisher LSD)

Table S1) were PCR-amplified, and the final PCR products were run on a 1.5% agarose gel, purified with Wizard SV Gel and PCR Clean-Up System (Promega, Madison, WI) and then sequenced following standard Sanger method. The electropherograms were analyzed with Mutation Surveyor software (Softgenetics, State College, PA) to determine the percentage of methylation for every cytosine residue.

Allele-specific expression assay

A custom TaqMan SNP Genotyping assay (Applied Biosystems) was designed to discriminate N28 and C22-4 alleles at *ZmRap2.7*. To produce a standard curve, genomic DNAs of N28 and C22-4 were mixed with the following ratios: 4:1, 3:1, 2:1, 1:1, 1:2, 1:3, and 1:4 (N28 allele/C22-4 allele). Following the manufacturer's protocol, PCRs were performed on these DNA mixes; the log of [FAM intensity (C22-4 allele)/VIC intensity (N28 allele)] was calculated at the last PCR cycle (cycle 40). The standard curve was then generated by linear regression ($y = a + bx$), where y is the log of (FAM intensity/VIC intensity) at a given mixing ratio, x is the log of mixing ratio, a is the intercept, and b is the slope. After RNA extraction from the leaves of N28xC22-4 F_1 hybrids with the TRI Reagent (Sigma-Aldrich) and cDNA synthesis with the High Capacity cDNA Reverse Transcription Kit (Applied Biosystems), PCRs using the custom TaqMan SNP were performed on cDNA samples; the allele ratio was calculated by intercepting log of (FAM intensity/VIC intensity) on the standard curve (Lo *et al.* 2003).

RESULTS

Temporal profile of *ZmRap2.7* expression

Leaf tissues sampled at four different developmental time points (V1, V3, V5, and V7) were used to determine *ZmRap2.7* expression by means of qPCR in five different maize lines: B73, N28, R22 (late flowering, carrying the late *Vgt1* allele) and Gaspé Flint and C22-4 (early flowering, early *Vgt1* allele). The lines B73, N28, and R22, carrying the late *Vgt1* allele, shared a common expression trend, characterized by a peak of *ZmRap2.7* expression at the stage V3, followed by a drop in the levels of *ZmRap2.7* transcripts in ensuing stages (Figure 1). Differently, C22-4 and Gaspé Flint showed maximum *ZmRap2.7* expression at V1. At V3, expression was significantly higher (Fisher's LSD test $P < 0.05$) in N28 compared with R22 and B73, whose expression levels were in turn significantly greater than in C22-4 and Gaspé Flint.

Bisulfite sequencing of portions of *Vgt1* in N28 and C22-4 reveals differential methylation and methylation spreading From the MITE transposon

To investigate the dynamics of *Vgt1* DNA methylation levels, we performed a preliminary analysis based on restriction with the methylation-dependent enzyme *Mcr*BC followed by qPCR, which showed a constant in time methylation peak in the central region of *Vgt1*. However, the analysis did not show any methylation difference between the early and late alleles (see File S1, Figure S1, Figure S2, Figure S3, Figure S4, Figure S5, Figure S6). Given the results obtained with this approach, we moved to bisulfite-based methylation analysis. We first focused on the *Vgt1* region encompassing the nucleotides 1570−1921 (Ampl bis-Sanger, see Figure 2). The results showed that the C22-4 (early) *Vgt1* allele is completely unmethylated at all developmental stages, because 54 of the 54 cytosines in the investigated region were converted to thymine. Conversely, for the N28 allele, a single cytosine residue (C-1761) was progressively more methylated during development (10% at stage V1, 16.7% at V3, 30.8% at V5, and 61.5% at V7) (Figure 3).

We next investigated a region surrounding the CNS sequence (for the N28 allele, 617−920 bp) or the CNS/MITE insertion (for the C22-4 allele, 292 bp corresponding to the sequence 643−792 bp of the N28 allele plus the MITE) (Figure 3). In both alleles, the region upstream the CNS or CNS/MITE insertion was scarcely methylated; cytosine methylation of the CNS sequence (743−761 bp) was extremely low (1.1%) whereas the MITE itself showed a very high level (85.8%) of average methylation (Average methylation for the three cytosine contexts: 88.8% CG, 89.0% CHG and 85.0% CHH) (Figure 4). N28 and C22-4 showed significant methylation differences among developmental stages; in particular, methylation of the N28 region was higher at V3, compared with earlier and later stages, whereas for C22-4 the

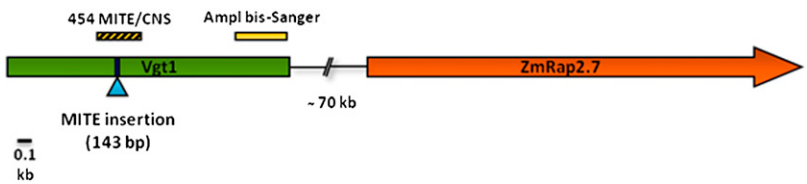

Figure 2 Schematic representation of the *Vgt1-ZmRap2.7* locus (Salvi *et al.* 2007) and of the polymerase chain reaction amplicons used for the bisulfite sequencing DNA methylation analysis. MITE, miniature transposon.

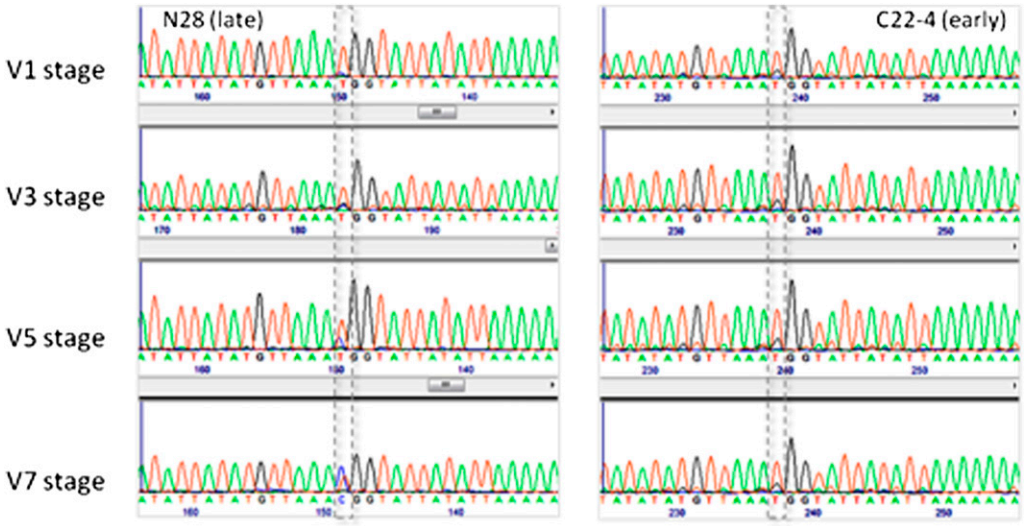

Figure 3 Portion of bisulfite sequencing (Sanger) chromatograms for the 'Ampl bis-Sanger' amplicon (1570−1921 bp) showing the differentially methylated cytosine C-1761.

most methylated stage corresponded to V7 ($P < 0.01$). The N28 and C22-4 amplicons overlap for 149 nucleotides and among the 31 shared cytosines, 11 showed a significantly different degree of methylation between N28 and C22-4 ($P < 0.01$). Interestingly, the four shared cytosines included in the CNS sequence were differentially methylated between N28 and C22-4 and significantly higher methylation was observed in C22-4 ($P < 0.01$) (Figure 4 and Figure S7).

Methylation patterns at *Vgt1* are stably maintained

Allele specific methylation analysis of the CNS/MITE region was determined at four developmental stages (V1, V3, V5, and V7) in F_1 plants obtained by crossing N28 and C22-4. The pattern of methylation of the two allelic forms strongly resembled what was observed in the parental inbred lines: the region upstream the MITE insertion (for the C22-4 allele) or the CNS sequence (in N28) showed weak methylation

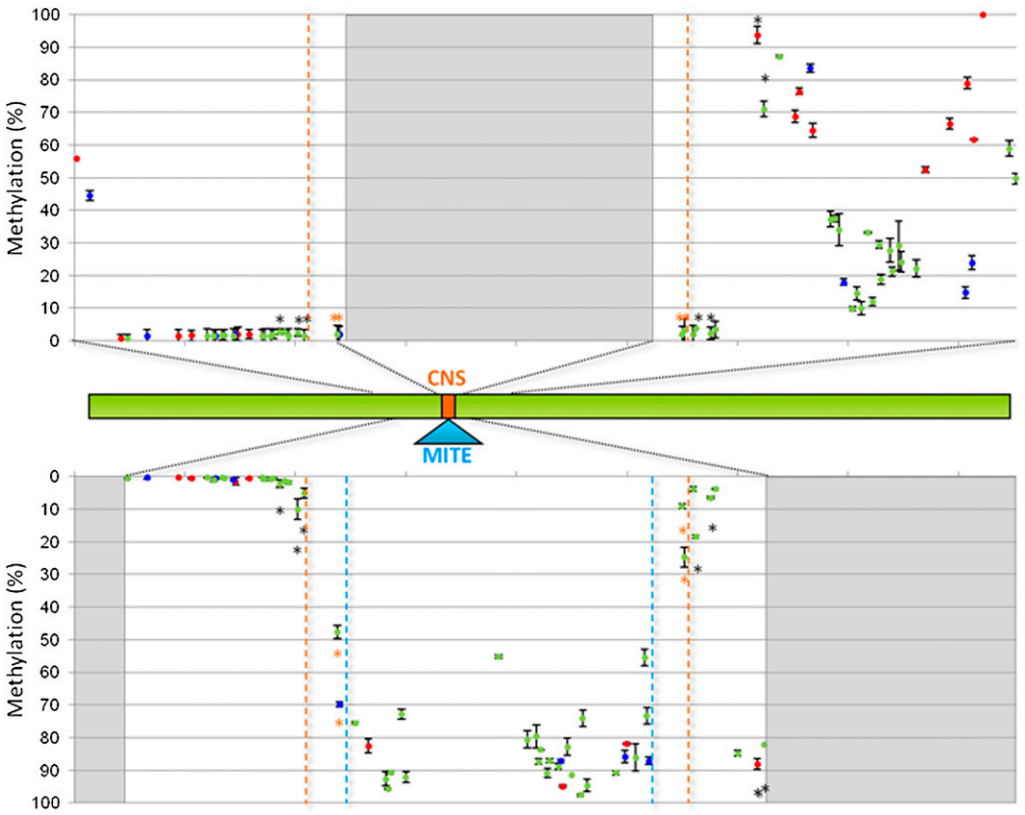

Figure 4 Results of the ultra-deep amplicon bisulfite sequencing at the conserved noncoding sequence/miniature transposon (CNS/MITE) region for the lines N28 and C22-4 at the V3 stage. Mean values are shown; standard deviation values are shown as bars. Methylation data points are represented in different colors, according to cytosine context: red for CG, blue for CHG, green for CHH. Top: methylation level (% of cytosine methylation as estimated by the Kismeth software, black vertical bars) for each cytosine within the sequence 617−920 bp of the N28 (late) allele. The gray block represents the site of MITE insertion (not present in the N28 allele). The orange dotted lines highlight the CNS sequence. Middle: the green bar represents the N28-*Vgt1* locus, with black dotted lines indicating the regions for which methylation has been explored in this experiment. Bottom: methylation level estimated for each cytosine of the C22-4 (early) allele within the region corresponding to the sequence 643−792 bp of the N28 allele. The gray blocks define regions within *Vgt1* that have not been tested in this analysis for the C22-4 allele with respect to N28. The light blue dotted lines delimitate the MITE insertion, which is present in C22-4 only. The black * indicates a significantly differentially methylated cytosine between N28 and C22-4 ($P < 0.01$, LSD). The orange * indicates significant difference in methylation at the cytosine included in the CNS region.

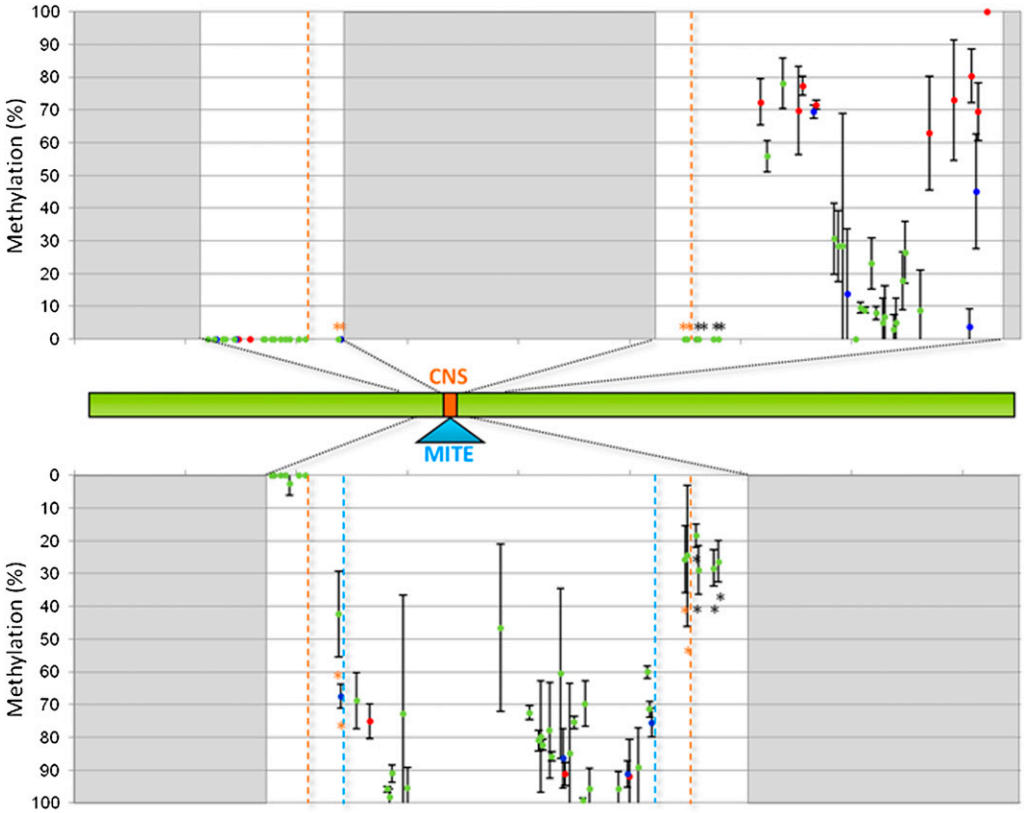

Figure 5 Results of the Sanger bisulfite sequencing at the CNS/MITE region within *Vgt1* for the N28xC22-4 F_1 hybrid line at the V3 stage. Mean values are shown; standard deviation values are shown as bars. Methylation data points are represented in different colors, according to cytosine context: red for CG, blue for CHG, green for CHH. Top: methylation level (% of cytosine methylation as estimated by the Mutation Surveyor software, black vertical bars) estimated for each cytosine of the N28 (late) allele. Middle: the green bar represents the N28-*Vgt1* locus with black dotted lines indicating the regions for which methylation has been explored in this experiment. Bottom: methylation level estimated for each cytosine of the C22-4 (early) allele. The two light blue dotted lines indicate the MITE insertion; the orange dotted lines highlight the CNS sequence. The black * indicates a significantly differentially methylated cytosine between N28 and C22-4 ($P < 0.01$, two tailed *t*-test). The orange * indicates a significant difference in methylation at the cytosine included in the CNS region. CNS/MITE, conserved noncoding sequence/miniature transposon.

and the CNS was completely unmethylated (0%), whereas cytosines in all the three possible context were heavily methylated within the MITE transposon (average 84.6% with 85.1% CG, 88.7% CHG, and 84.0% CHH) (Figure 5 and Figure S8). Among the 26 cytosines shared between the two alleles and surveyed in this experiment, eight are more methylated in the C22-4 allele (two tailed *t*-test, $P < 0.01$), this being more evident for the residues adjacent to the MITE transposon. The four cytosines within the CNS displayed a higher level of methylation in C22-4 ($P < 0.01$), as observed in the inbred line-based experiment.

ZmRap2.7 allele-specific expression assay

In a previous work, *Vgt1* was shown to be a *cis*-regulator of *ZmRap2.7* transcription (Salvi *et al.* 2007). To test the correlation between cytosine methylation at *Vgt1* and expression of the two alleles of *ZmRap2.7*, we performed an allele-specific TaqMan expression assay on the same N28 × C22-4 F_1 plants analyzed for methylation. At all stages, the N28 transcript was more abundant than C22-4; moreover, the ratio of allele expression N28/C22-4 significantly increased during development (two-tailed *t*-test, $P < 0.05$. Table 1).

Methylation at the CNS within *Vgt1* is conserved between maize and sorghum

By means of bisulfite sequencing, we analyzed cytosine methylation at the sorghum 438-bp region including the CNS sequence which is syntenic to the maize *Vgt1*-associated CNS. DNA methylation was notably low at the four cytosines contained in the CNS itself (2.1%, on average) and at nearby cytosines, with values comparable with those detected at the CNS in N28 (1.1%). Moving away from the CNS, the level of methylation increased substantially on both sides (Figure 6 and Figure S9). Comparing the two stages of development, we observed that average methylation was higher in the V7 phase ($P < 0.01$).

DISCUSSION

Vgt1 pattern of methylation

Methylation analysis at *Vgt1* revealed that the N28 (late) and C22-4 (Gaspé Flint-originated, early) alleles differ significantly in cytosine methylation patterns. In particular, sequencing of the region encompassing the CNS/MITE sequence showed that the MITE transposon is heavily methylated and that this state is also present (at least at short

Table 1 Allele-specific expression assay

	First Leaf	Third Leaf	Fifth Leaf	Seventh Leaf
N28 expression proportion	0.52 (a)	0.57 (ab)	0.61 (b)	0.62 (b)

Results of allele specific expression assay, performed on the N28xC22-4 F1 hybrid line at four developmental stages. The values represent the proportion of the N28 allele transcript abundance over C22-4 transcript abundance. Different letters (a−b) indicate significant difference ($P < 0.01$, Fisher LSD). Letters shared between two groups (*i.e.*, a, ab) indicate a nonsignificant difference.

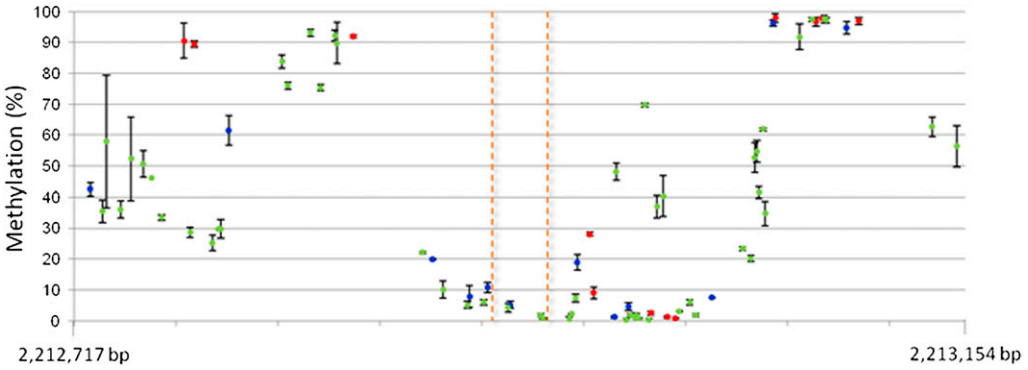

Figure 6 Results of the ultra-deep amplicon bisulfite sequencing of a region spanning the nucleotides 2,212,717 - 2,213,154 on sorghum chromosome 9 (JGI, v1.4) surrounding the CNS sequence in sorghum B.Tx623 at the V1 stage. On the y-axis, % of cytosine methylation as estimated by the Kismeth software. Methylation data points (mean values) are represented in different colors, according to cytosine context: red for CG, blue for CHG, green for CHH. The orange dotted lines highlight the CNS sequence. CNS, conserved noncoding sequence.

distance) at cytosine residues lying outside the boundaries of the TE itself, including cytosines belonging to the CNS sequence in the early *Vgt1* allele. Furthermore, the methylation state of the two alleles is stably maintained, as the methylation pattern of single alleles did not change when assayed in F_1 hybrid plants.

MITE insertions can alter methylation at adjacent sites and impact gene expression

MITE transposon insertions such as the one observed at *Vgt1* have been repeatedly shown to be associated with QTL for agronomic traits in crops (Guillet-Claude *et al.* 2004; Magalhaes *et al.* 2007; Studer *et al.* 2011; Hou *et al.* 2012; Zerjal *et al.* 2012). In most cases, the MITE insertion seemed to act by disrupting a regulatory element of a nearby gene. The detailed molecular mechanisms by which a MITE insertion affects gene expression have not been elucidated and could include, besides the interruption of a transcription factor recognition sequence, the production of stable secondary chromatin structure (Bureau and Wessler 1992) and/or change in chromatin state due the action of siRNA, as shown by the fact that MITEs can be both target and source of siRNA (Kuang *et al.* 2009; Lu *et al.* 2011). Methylation changes induced by siRNA could also directly or indirectly affect the expression of nearby genes.

In plants, small interfering heterochromatic RNAs (24 nt in length) are involved in the formation of heterochromatin by guiding the action of the RNAi machinery against target DNA sequences (typically repeats and transposable elements), which as a result become methylated (Matzke *et al.* 2007; Daxinger *et al.* 2009; Hale *et al.* 2009; Simon and Meyers 2011). We looked for siRNA potentially targeting the *Vgt1* region using available small RNA libraries from the inbred line B73 (GEO accession number GSE17339) and the *mop1-1* mutant (GEO accession number GSE12173) (Nobuta *et al.* 2008); we aligned the reads using both *Vgt1* N28 and *Vgt1* C22-4 as reference sequences. A negligible number of hits were found when *Vgt1* N28 was the reference. As an example, with the B73 tassel library we observed that 1537 of the 1786 distinct sequences matching *Vgt1* C22-4 are 24-mers reads. In particular, the reads corresponding to the small RNA AAUCCACAUGGAUUGAGAGCUAAC, whose putative target sequence lies within the MITE transposon, represent over half of the sequences aligning against *Vgt1* C22-4. As expected, the abundance of such 24-mer is dramatically reduced in the *mop1-1* mutant. A siRNA directed against the same sequence was found to potentially target another MITE whose insertion at the *ZmV1-9* locus on chromosome 1 is associated to late male flowering phenotypes (Zerjal *et al.* 2012). This small RNA has hundreds of matches to many genomic locations, which precludes establishing an unambiguous connection to the *Vgt1* locus. This notwithstanding, it might play an important role in silencing and in accordance with our results we hypothesize that the binding of the small RNA is responsible for the heavy methylation of its target site within *Vgt1* and possibly of the methylation spreading to the adjacent sequences. As a supporting evidence to this hypothesis, our data showed that asymmetric CHH methylation, which is established and maintained via the RdDM pathway (Law and Jacobsen 2010), is extremely high across the MITE transposon.

Spreading of methylation from the MITE insertion to other regulatory sequences could be part of the molecular mechanism involved in translating the effect of MITE insertion in promoters and/or enhancers of *Vgt1*. In fact, heterochromatin spreading has been proposed as one of the mechanisms impacting gene regulation on a genome-wide scale as a consequence of transposon insertion in maize (Eichten *et al.* 2011).

Propagation of DNA methylation from transposons to adjacent regulatory sequences has been observed for at least another locus in maize, the *p1* gene, which is involved in the biosynthesis of phlobaphene pigments (Grotewold *et al.* 1994). In this case, the differential expression of the two epialleles *P1-rr* and *P1-pr* appears to arise from different cytosine methylation patterns at a distal enhancer located upstream the TSS, caused by a leakage of methylation from the hypermethylated nearby hAT and MULE elements that affects only the *P1-pr* silenced allele (Goettel and Messing 2013). Interestingly, also in this example spreading of methylation seemed to occur from transposons belonging to the MITE family, although this phenomenon did not contribute to obvious phenotypic variation.

A complex network controls *ZmRap2.7* expression

The lack of a perfect correlation between levels of *ZmRap2.7* gene expression and genotype (and methylation state) at *Vgt1* is likely due to the complexity of *ZmRap2.7* gene expression regulation. Indeed, besides *Vgt1*, *ZmRap2.7* expression is likely to be under control of miR172 (given the presence of miR172 target sequence in *ZmRap2.7*), one of the most important and evolutionary ancient noncoding microRNAs (Park *et al.* 2002; Chen 2004), which seems to act by targeting mRNAs both by cleavage and translational repression (Zhu and Helliwell

2011). In our case, a different genotypic architecture for the miR172 family among B73 (five miR172 loci are present in the B73 genome. Zhu and Helliwell 2011), N28 and R22 could be responsible for differential effects on *ZmRap2.7* expression. Additionally, the expression of *ZmRap2.7* could be under feedback regulation as shown for the related gene *AP-2* in Arabidopsis (Schwab *et al.* 2005). Moreover, in addition to the CNS/MITE region, other sites within *Vgt1* might as well be involved in controlling *ZmRap2.7* expression: indeed, our results highlight at least one site, nucleotide C-1761, that shows not only differential methylation between the two alleles but also an increasing methylation during development in the N28 allele.

Evolutionary conserved sequences share common features

Vgt1-ZmRap2.7 was previously shown to correspond to a syntenic flowering time QTL in sorghum (short arm of chr. 9) with relatively high map resolution (1.9 cM, Mace *et al.* 2013; see also Brown *et al.* 2006 and Feltus *et al.* 2006). We previously found that a CNS was shared between maize *Vgt1* and the syntenic region in sorghum and rice (Salvi *et al.* 2007). Our methylation results now showed that the maize and sorghum *Vgt1*-related CNSs shared the same hypomethylation profile relative to surrounding regions, a distinguished feature of chromatin regions involved in the binding of transcription factors (Stadler *et al.* 2011; Thurman *et al.* 2012). Moreover, a survey of the DNA methylation maps of four rice cultivars (Li *et al.* 2012) revealed that a similar pattern of low methylation characterizes the CNS in this species as well (not shown).

A model for *Vgt1* regulation of *ZmRap2.7* expression

Although our results do not provide conclusive evidence of a causal connection between differential methylation and *Vgt1* effect, they show a clear association between the MITE transposon insertion and hypermethylation at *Vgt1*. Based on these results, we propose a model in which, in the Gaspé-Flint allele, (i) the interruption of the CNS sequence by the insertion of the MITE transposon, (ii) the hypermethylation resulting from the presence of the MITE, or (iii) a combination of both these features can influence the interaction between *Vgt1* and *ZmRap2.7*. This alteration, in early stages of development prior to meristem transition, could reduce *ZmRap2.7* transcription, which eventually leads to early flowering. Further experimental evidence is needed to support the present hypothesis. One possibility is to investigate *Vgt1* function in an altered methylation context (*e.g.*, by the use of mutants in the methylation machinery, and/or by chemical modulators. Baubec *et al.* 2009; Law and Jacobsen 2010). Additionally, the study of DHS (DNaseI hypersensitivity) (Cockerill 2011) and histone modifications such as dimethylation of H3 lysine 9 or trimethylation of H3 lysine 27 (Locatelli *et al.* 2009) in the *Vgt1-ZmRap2.7* region would help to clarify if differential methylation observed at the two alleles is related to the level of chromatin compaction at *Vgt1* and how this state could be transmitted to the *ZmRap2.7* locus. The study of the three-dimensional architecture of the *Vgt1-ZmRap2.7* locus and long-range interactions between DNA sequences by chromosome conformation capture (Louwers *et al.* 2009; Crevillén *et al.* 2013) could also contribute to the understanding of the mechanism of action of *Vgt1*.

ACKNOWLEDGMENTS

We thank Simona Corneti, Emanuele De Paoli, Jun Lv, Luca Morandi, Vincenzo Rossi, Maria Corinna Sanguineti, Riccardo Velasco, and Wen Wang for technical support and Blake Meyers, Scott A. Jackson, and Clémentine Vitte for technical support and useful comments on an earlier version of this manuscript.

LITERATURE CITED

Arteaga-Vazquez, M., L. Sidorenko, F. A. Rabanal, R. Shrivistava, K. Nobuta *et al.*, 2010 RNA-mediated trans-communication can establish paramutation at the b1 locus in maize. Proc. Natl. Acad. Sci. USA 107: 12986–12991.

Baubec, T., A. Pecinka, W. Rozhon, and O. Mittelsten Scheid, 2009 Effective, homogeneous and transient interference with cytosine methylation in plant genomic DNA by zebularine. Plant J. 57: 542–554.

Brink, R., 1958 Paramutation at the R-locus in maize. Cold Spring Harb. Symp. Quant. Biol. 23: 379–391.

Brown, P. J., P. E. Klein, E. Bortiri, C. B. Acharya, W. L. Rooney *et al.*, 2006 Inheritance of inflorescence architecture in sorghum. Theor. Appl. Genet. 113: 931–942.

Buckler, E. S., J. B. Holland, P. J. Bradbury, C. B. Acharya, P. J. Brown *et al.*, 2009 The genetic architecture of maize flowering time. Science 325: 714–718.

Bureau, T. E., and S. R. Wessler, 1992 Tourist: a large family of small inverted repeat elements frequently associated with maize genes. Plant Cell 4: 1283–1294.

Chardon, F., B. Virlon, L. Moreau, M. Falque, J. Joets *et al.*, 2004 Genetic architecture of flowering time in maize as inferred from quantitative trait loci meta-analysis and synteny conservation with the rice genome. Genetics 168: 2169–2185.

Chen, X., 2004 A microRNA as a translational repressor of APETALA2 in Arabidopsis flower development. Science 303: 2022–2025.

Cockerill, P. N., 2011 Structure and function of active chromatin and DNase I hypersensitive sites. FEBS J. 278: 2182–2210.

Cokus, S. J., S. Feng, X. Zhang, Z. Chen, B. Merriman *et al.*, 2008 Shotgun bisulphite sequencing of the Arabidopsis genome reveals DNA methylation patterning. Nature 452: 215–219.

Crevillén, P., C. Sonmez, Z. Wu, and C. Dean, 2013 A gene loop containing the floral repressor FLC is disrupted in the early phase of vernalization. EMBO J. 32: 140–148.

Cubas, P., C. Vincent, and E. Coen, 1999 An epigenetic mutation responsible for natural variation in floral symmetry. Nature 401: 157–161.

Daxinger, L., T. Kanno, E. Bucher, J. Van Der Winden, U. Naumann *et al.*, 2009 A stepwise pathway for biogenesis of 24-nt secondary siRNAs and spreading of DNA methylation. EMBO J. 28: 48–57.

Ducrocq, S., D. Madur, J.-B. Veyrieras, L. Camus-Kulandaivelu, M. Kloiber-Maitz *et al.*, 2008 Key impact of *Vgt1* on flowering time adaptation in maize: evidence from association mapping and ecogeographical information. Genetics 178: 2433–2437.

Eichten, S. R., R. A. Swanson-Wagner, J. C. Schnable, A. J. Waters, P. J. Hermanson *et al.*, 2011 Heritable epigenetic variation among maize inbreds. PLoS Genet. 7: e1002372.

Feltus, F. A., G. E. Hart, K. F. Schertz, A. M. Casa, S. Kresovich *et al.*, 2006 Alignment of genetic maps and QTLs between inter- and intra-specific sorghum populations. Theor. Appl. Genet. 112: 1295–1305.

Feng, S., S. E. Jacobsen, and W. Reik, 2010 Epigenetic reprogramming in plant and animal development. Science 330: 622–627.

Freeling, M., and S. Subramaniam, 2009 Conserved noncoding sequences (CNSs) in higher plants. Curr. Opin. Plant Biol. 12: 126–132.

Gent, J. I., N. A. Ellis, L. Guo, A. E. Harkess, Y. Yao *et al.*, 2013 CHH islands: de novo DNA methylation in near-gene chromatin regulation in maize. Genome Res. 23: 628–637.

Goettel, W., and J. Messing, 2013 Epiallele biogenesis in maize. Gene 516: 8–23.

Grotewold, E., B. J. Drummond, B. Bowen, and T. Peterson, 1994 The myb-homologous P gene controls phlobaphene pigmentation in maize floral organs by directly activating a flavonoid biosynthetic gene subset. Cell 76: 543–553.

Gruntman, E., Y. Qi, R. K. Slotkin, T. Roeder, R. A. Martienssen *et al.*, 2008 Kismeth: Analyzer of plant methylation states through bisulfite sequencing. BMC Bioinformatics 9: 371.

Guillet-Claude, C., C. Birolleau-Touchard, D. Manicacci, P. M. Rogowsky, J. Rigau *et al.*, 2004 Nucleotide diversity of the ZmPox3 maize peroxidase gene: Relationships between a MITE insertion in exon 2 and variation in forage maize digestibility. BMC Genet. 5: 19.

Hale, C. J., K. F. Erhard, D. Lisch, and J. B. Hollick, 2009 Production and processing of siRNA precursor transcripts from the highly repetitive maize genome. PLoS Genet. 5: 14.

Hou, J., Y. Long, H. Raman, X. Zou, J. Wang *et al.*, 2012 A Tourist-like MITE insertion in the upstream region of the BnFLC.A10 gene is associated with vernalization requirement in rapeseed (Brassica napus L.). BMC Plant Biol. 12: 238.

Hung, H. Y., L. M. Shannon, F. Tian, P. J. Bradbury, C. Chen *et al.*, 2012 ZmCCT and the genetic basis of day-length adaptation underlying the postdomestication spread of maize. Proc. Natl. Acad. Sci. USA 109: E1913–E1921.

Johannes, F., E. Porcher, F. K. Teixeira, V. Saliba-Colombani, M. Simon *et al.*, 2009 Assessing the impact of transgenerational epigenetic variation on complex traits. PLoS Genet. 5: 11.

Jones, P. A., 2012 Functions of DNA methylation: islands, start sites, gene bodies and beyond. Nat. Rev. Genet. 13: 484–492.

Kuang, H., C. Padmanabhan, F. Li, A. Kamei, P. B. Bhaskar *et al.*, 2009 Identification of miniature inverted-repeat transposable elements (MITEs) and biogenesis of their siRNAs in the Solanaceae: new functional implications for MITEs. Genome Res. 19: 42–56.

Law, J. A., and S. E. Jacobsen, 2010 Establishing, maintaining and modifying DNA methylation patterns in plants and animals. Nat. Rev. Genet. 11: 204–220.

Li, X., J. Zhu, F. Hu, S. Ge, M. Ye *et al.*, 2012 Single-base resolution DNA methylomes of rice and new regulatory roles of DNA methylation in plant gene expression. BMC Genomics 13: 300.

Lippman, Z., B. May, C. Yordan, T. Singer, and R. Martienssen, 2003 Distinct mechanisms determine transposon inheritance and methylation via small interfering RNA and histone modification. PLoS Biol. 1: E67.

Lister, R., R. C. O'Malley, J. Tonti-Filippini, B. D. Gregory, C. C. Berry *et al.*, 2008 Highly integrated single-base resolution maps of the epigenome in Arabidopsis. Cell 133: 523–536.

Livak, K. J., and T. D. Schmittgen, 2001 Analysis of relative gene expression data using real-time quantitative PCR and the $2-\Delta\Delta CT$ method. Methods 25: 402–408.

Lo, H. S., Z. Wang, Y. Hu, H. H. Yang, S. Gere *et al.*, 2003 Allelic variation in gene expression is common in the human genome. Genome Res. 13: 1855–1862.

Locatelli, S., P. Piatti, M. Motto, and V. Rossi, 2009 Chromatin and DNA modifications in the Opaque2-mediated regulation of gene transcription during maize endosperm development. Plant Cell 21: 1410–1427.

Louwers, M., R. Bader, M. Haring, R. Van Driel, W. De Laat *et al.*, 2009 Tissue- and expression level-specific chromatin looping at maize b1 epialleles. Plant Cell 21: 832–842.

Lu, C., J. Chen, Y. Zhang, Q. Hu, W. Su *et al.*, 2011 Miniature inverted-repeat transposable elements (MITEs) have been accumulated through amplification bursts and play important roles on gene expression and species diversity in Oryza sativa. Mol. Biol. Evol. 29: 1005–1017.

Mace, E. S., C. H. Hunt, and D. R. Jordan, 2013 Supermodels: sorghum and maize provide mutual insight into the genetics of flowering time. Theor. Appl. Genet. 126: 1377–1395.

Magalhaes, J. V., J. Liu, C. T. Guimarães, U. G. P. Lana, V. M. C. Alves *et al.*, 2007 A gene in the multidrug and toxic compound extrusion (MATE) family confers aluminum tolerance in sorghum. Nat. Genet. 39: 1156–1161.

Martin, A., C. Troadec, A. Boualem, M. Rajab, R. Fernandez *et al.*, 2009 A transposon-induced epigenetic change leads to sex determination in melon. Nature 461: 1135–1138.

Matzke, M., T. Kanno, B. Huettel, L. Daxinger, and A. J. M. Matzke, 2007 Targets of RNA-directed DNA methylation. Curr. Opin. Plant Biol. 10: 512–519.

Nobuta, K., C. Lu, R. Shrivastava, M. Pillay, E. De Paoli *et al.*, 2008 Distinct size distribution of endogeneous siRNAs in maize: Evidence from deep sequencing in the mop1–1 mutant. Proc. Natl. Acad. Sci. USA 105: 14958–14963.

Park, W., J. Li, R. Song, J. Messing, and X. Chen, 2002 CARPEL FACTORY, a Dicer homolog, and HEN1, a novel protein, act in microRNA metabolism in *Arabidopsis thaliana*. Curr. Biol. 12: 1484–1495.

Phillips, R., T. Kim, S. Kaeppler, S. Parentoni, D. Shaver *et al.*, 1992 Genetic dissection of maturity using RFLP vol. 47, pp. 135–150. in Proceedings 47th Annual Corn and Sorghum Research Conference, Chicago.

Ritchie, S. W., J. J. Hanway, and G. O. Benson, 1993 How A Corn Plant Develops. Special Report No. 48 Cooperative Extension Service. Iowa State University, Ames, Iowa.

Saghai-Maroof, M. A., K. M. Soliman, R. A. Jorgensen, and R. W. Allard, 1984 Ribosomal DNA spacer-length polymorphisms in barley: mendelian inheritance, chromosomal location, and population dynamics. Proc. Natl. Acad. Sci. USA 81: 8014–8018.

Salvi, S., R. Tuberosa, E. Chiapparino, M. Maccaferri, S. Veillet *et al.*, 2002 Toward positional cloning of Vgt1, a QTL controlling the transition from the vegetative to the reproductive phase in maize. Plant Mol. Biol. 48: 601–613.

Salvi, S., G. Sponza, M. Morgante, D. Tomes, X. Niu *et al.*, 2007 Conserved noncoding genomic sequences associated with a flowering-time quantitative trait locus in maize. Proc. Natl. Acad. Sci. USA 104: 11376–11381.

Salvi, S., S. Castelletti, and R. Tuberosa, 2009 An updated consensus map for flowering time QTLs in maize. Maydica 54: 501–512.

Schnable, P. S., D. Ware, R. S. Fulton, J. C. Stein, F. Wei *et al.*, 2009 The B73 maize genome: complexity, diversity, and dynamics. Science 326: 1112–1115.

Schwab, R., J. F. Palatnik, M. Riester, C. Schommer, M. Schmid *et al.*, 2005 Specific effects of microRNAs on the plant transcriptome. Dev. Cell 8: 517–527.

Simon, S. A., and B. C. Meyers, 2011 Small RNA-mediated epigenetic modifications in plants. Curr. Opin. Plant Biol. 14: 148–155.

Stadler, M. B., R. Murr, L. Burger, R. Ivanek, F. Lienert *et al.*, 2011 DNA-binding factors shape the mouse methylome at distal regulatory regions. Nature 480: 490–495.

Stam, M., C. Belele, J. E. Dorweiler, and V. L. Chandler, 2002 Differential chromatin structure within a tandem array 100 kb upstream of the maize b1 locus is associated with paramutation. Genes Dev. 16: 1906–1918.

Studer, A., Q. Zhao, J. Ross-Ibarra, and J. Doebley, 2011 Identification of a functional transposon insertion in the maize domestication gene tb1. Nat. Genet. 43: 1160–1163.

Telias, A., K. Lin-Wang, D. E. Stevenson, J. M. Cooney, R. P. Hellens *et al.*, 2011 Apple skin patterning is associated with differential expression of MYB10. BMC Plant Biol. 11: 93.

Thurman, R. E., E. Rynes, R. Humbert, J. Vierstra, M. T. Maurano *et al.*, 2012 The accessible chromatin landscape of the human genome. Nature 489: 75–82.

Truntzler, M., N. Ranc, M. C. Sawkins, S. Nicolas, D. Manicacci *et al.*, 2012 Diversity and linkage disequilibrium features in a composite public/private dent maize panel: consequences for association genetics as evaluated from a case study using flowering time. Theor. Appl. Genet. 125: 731–747.

Tuberosa, R., and S. Salvi, 2009 QTL for agronomic traits in maize production, pp. 501–542 in *Handbook of Maize: Its Biology*, edited by J. L. Bennetzen, and S. C. Hake. Springer, New York.

Vlăduţu, C., J. McLaughlin, and R. L. Phillips, 1999 Fine mapping and characterization of linked quantitative trait loci involved in the transition of the maize apical meristem from vegetative to generative structures. Genetics 153: 993–1007.

Wei, F., E. Coe, W. Nelson, A. K. Bharti, F. Engler *et al.*, 2007 Physical and genetic structure of the maize genome reflects its complex evolutionary history. PLoS Genet. 3: 10.

Woodhouse, M. R., M. Freeling, and D. Lisch, 2006 The mop1 (mediator of paramutation1) mutant progressively reactivates one of the two genes encoded by the MuDR transposon in maize. Genetics 172: 579–592.

Zemach, A., I. E. McDaniel, P. Silva, and D. Zilberman, 2010 Genome-wide evolutionary analysis of eukaryotic DNA methylation. Science 328: 916–919.

Zerjal, T., A. Rousselet, C. Mhiri, V. Combes, D. Madur *et al.*, 2012 Maize genetic diversity and association mapping using transposable element insertion polymorphisms. Theor. Appl. Genet. 124: 1521–1537.

Zhang, M., J. N. Kimatu, K. Xu, and B. Liu, 2010 DNA cytosine methylation in plant development. J. Genet. Genomics 37: 1–12.

Zhang, X., J. Yazaki, A. Sundaresan, S. Cokus, S. W.-L. Chan *et al.*, 2006 Genome-wide high-resolution mapping and functional analysis of DNA methylation in Arabidopsis. Cell 126: 1189–1201.

Zhu, Q.-H., and C. A. Helliwell, 2011 Regulation of flowering time and floral patterning by miR172. J. Exp. Bot. 62: 487–495.

Zilberman, D., M. Gehring, R. K. Tran, T. Ballinger, and S. Henikoff, 2007 Genome-wide analysis of *Arabidopsis thaliana* DNA methylation uncovers an interdependence between methylation and transcription. Nat. Genet. 39: 61–69.

Communicating editor: J. A. Birchler